Food and Chemical Toxicology 73 (2014) 105–112

Contents lists available at ScienceDirect

Food and Chemical Toxicology

journal homepage: www.elsevier.com/locate/foodchemtox

Evaluation of in vitro cytotoxicity and genotoxicity of copper–zinc alloy nanoparticles in human lung epithelial cells

Ümit Kumbıçak [a], Tolga Çavaş [b,*], Nilüfer Çinkılıç [b], Zübeyde Kumbıçak [a], Özgür Vatan [b], Dilek Yılmaz [b]

[a] Department of Molecular Biology and Genetics, Faculty of Science and Art, Nevşehir University, 50300 Nevşehir, Turkey
[b] Cell Culture and Genetic Toxicology Laboratory, Department of Biology, Faculty of Sciences and Arts, Uludağ University, 16059 Nilüfer, Bursa, Turkey

ARTICLE INFO

Article history:
Received 15 March 2014
Accepted 31 July 2014
Available online 10 August 2014

Keywords:
Nanotoxicology
Copper–zinc alloy nanoparticles
BEAS-2B cells
Cytotoxicity
Genotoxicity

ABSTRACT

In the present study, in vitro cytotoxic and genotoxic effect of copper–zinc alloy nanoparticles (Cu–Zn ANPs) on human lung epithelial cells (BEAS-2B) were investigated. XTT test and clonogenic assay were used to determine cytotoxic effects. Cell death mode and intracellular reactive oxygen species formations were analyzed using M30, M65 and ROS Elisa assays. Genotoxic effects were evaluated using micronucleus, comet and γ-H2AX foci assays. Cu–Zn ANPs were characterized by transmission electron microscopy (TEM), dynamic light scattering (DLS) and zeta potential measurements. Characterization of Cu–Zn ANPs showed an average size of 200 nm and zeta potential of −22 mV. TEM analyses further revealed the intracellular localization of Cu–Zn ANPs in cytoplasm within 24 h. Analysis of micronucleus, comet and γ-H2AX foci counts showed that exposure to Cu–Zn ANPs significantly induced chromosomal damage as well as single and double stranded DNA damage in BEAS-2B cells. Our results further indicated that exposure to Cu–Zn ANPs significantly induced intracellular ROS formation. Evaluation of M30:M65 ratios suggested that cell death was predominantly due to necrosis.

1. Introduction

In the last decade, significant progress has been achieved in the nano-scale science and technology. Today, nanomaterials and nanoparticles are widely used in different areas such as health, cosmetics, clothing, food, energy, space exploration, and defense industries (Arora et al., 2012; Ferreira et al., 2013). Among different types of nanoparticles, metals constitute one of the most widely studied groups due to their widespread usage. Most widely studied metal nanoparticles include gold, silver, titanium, and iron particles (Hussain et al., 2005; Schrand et al., 2010; Love et al., 2012). The widespread production and utilization of nanoparticles also makes them available for humans and the environment. Chemical, physical, and functional properties of nano-sized particles often differ compared with particles of larger size or dissolved species of the same element (Roduner, 2006). Similarly they can show different effects on biological systems then they exhibit on a macro-scale (Nel et al., 2006; Midander et al., 2009). It is known that, nanoparticles may lead the cell death via damaging DNA or organelles (Buzea et al., 2007; Manke et al., in press). Thus the evaluation of potential effects of nanoparticles is crucial.

In the recent years Copper and zinc containing nanoparticles also received considerable attention due to their unique antibacterial, antifungal, UV filtering and semiconductor properties as well as their high catalytic and photochemical activities (Meruvu et al., 2011; Trickler et al., 2012). In vivo studies demonstrated the toxicity of Cu and Zn containing nanoparticles on different organisms such as fish (Ateş et al., in press), drosophila (Han et al., 2014), amphipods (Hanna et al., 2013), rats (Amara et al., in press), mice (Adamcakova-Dodd et al., 2014) and bacteria (Rousk et al., 2012). In vitro toxicity of Cu Zn nanoparticles have also been shown by several authors (Akhtar et al., 2012; Chang et al., 2012; Sahu et al., 2013). In general, Cu and zinc Zn containing nanoparticles were found to be comparatively more toxic than other metal nanoparticles (Karlsson et al., 2008, 2013). For instance, Lanone et al. (2009) compared 24 different nanoparticles on the toxicity in the human lung cell line (A549) and macrophage cell line (THP-1) and found that copper and zinc containing nanoparticles were the most toxic ones, whereas titanium, aluminum, cerium, and zirconium containing nanoparticles were moderately toxic and tungsten carbide nanoparticles were non-toxic.

Metals can be mixed in different proportions to create new metallic systems with different characteristics (Ferrando et al., 2008). In this manner, combination of copper and zinc elements constitute a well-known example of metal alloys (Singh et al., 2009). Cu–Zn ANPs are one of the most commonly used alloys

* Corresponding author. Tel.: +90 224 2941869; fax: +90 224 2941899.
E-mail address: tcavas@uludag.edu.tr (T. Çavaş).

http://dx.doi.org/10.1016/j.fct.2014.07.040
0278-6915/

especially in biomedical applications and in consumer products, due to their specific properties (Tripathi et al., 2012; Bondarenko et al., 2013; Karlsson et al., 2013). They are also used during production stages of microbateries, microelectronic circuits, nanocables and nanoliquids (Tripathi et al., 2012). It is known that alloys can possess different effecs than their components (Bardack et al., 2014). Numerous genotoxicity studies have demonstrated DNA damaging potential of copper and zinc containing nanoparticles on human skin keratinocytes (Alarifi et al., 2013), lung epithelial cells (Ahamed et al., 2010), peripheral blood lymphocytes (Gumus et al., 2014) and kidney cells (Wahab et al., 2013). However, Cytotoxicity and genotoxicity data on the Cu–Zn ANPs is scarce.

In the present study, we aimed to evaluate the in vitro cytotoxic and genotoxic effects of Cu–Zn ANPs on human lung epithelium cells (BEAS-2B). We used XTT and clonogenic assays to assess cytotoxicity and comet, micronucleus (MN) and gamma H2AX foci formation assays to evaluate genotoxicity. Additionally, we measured the intracellular production of reactive oxygen species (ROS) by the oxidation sensitive fluoroprobe 2,7-dichlorofluorescin diacetate (DCFH-DA) and applied M30 and M65 assays to evaluate apoptotic and necrotic responses, respectively.

2. Materials and methods

2.1. Chemicals

Cu–Zn ANPs (40%Zn–60%Cu: <150 nm) at >99% purity were purchased from Sigma–Aldrich. Other chemicals and their sources were as follows: RPMI-1640 medium and supplemental growth factors (Lonza, Basel, Switzerland); PBS, cytochalasin-B, giemsa, low melting point agarose, normal melting point agarose, EDTA and Triton X-100 (Sigma–Aldrich, St. Louis, MO); anti phospho γ-H2AX primary and aleuxafuor 488 labeled secondary antibodies (Thermo Scientific and Invitrogen). Hydrogen peroxide (H_2O_2) was used as positive control at a single concentration of 147 μM. Sterile distilled water was used as solvent control at a maximum concentration of 0.5% (v/v).

2.2. Characterization of nanoparticles

A stock suspension of Cu–Zn ANPs (final concentration 1 mg/ml) was prepared in distilled water. Prior to each treatment, it was ultrasonicated (Bandelin Sonifier) for 20 min and diluted to prepare the desired ANPs concentrations. Particle morphology, size, and agglomeration states were characterized by using transmission electron microscopy (TEM), dynamic light scattering (DLS), and zeta potential analyses. Average hydrodynamic size, size distribution, and zeta potential of particles in suspension were determined by dynamic light scattering (DLS) using a Malvern Zetasizer.

2.3. Cell culture

Since inhalation is considered as one of the main routes of exposure to copper and zinc, healthy human lung epithelial cell line (BEAS-2B) was selected for out studies. Suitability of this cell line for genotoxicity assessment of different types of chemicals including nanoparticles has also been previously demonstrated (Capasso et al., 2014; Kim et al., 2011). BEAS-2B cells were kindly provided by Dr. E. Ulukaya (University of Uludağ). The cells were grown in RPMI-1640 medium supplemented with 10% fetal calf serum (FCS), penicillin–streptomycin (50 μg/ml), 2 mM L-glutamine, and 1% sodium pyruvate. Cells were maintained at 37 °C in a humidified atmosphere containing 5% CO_2 and grown in 75 cm^2 flasks and subcultured once a week.

2.4. Selection of the doses

BEAS-2B cells were exposed to serial concentrations of Cu–Zn ANPs (0.1, 0.5, 1, 5, 8, 12, 16, 20, 25, 50 and 100 μg/ml) to determine cytotoxicity and IC50 value. According to determined IC50 value, non-cytotoxic and low cytotoxic doses (0.1, 0.2, 0.4, 0.8, 1.6 and 3.2 μg/ml) of Cu–Zn ANPs were selected for genotoxicity experiments. Furthermore, two additional toxic doses (6.4 and 12.8 μg/ml) were also used to obtain and analyze cell death pathways in M30 and M65 tests.

2.5. Cellular uptake

BEAS-2B cells exposed to 2 μg/ml of ANPs solution for 24 h were examined under TEM to evaluate possible cellular internalization of Cu–Zn ANPs.

2.6. Cytotoxicity

XTT and clonogenic assays were used to test the potential effects of Cu–Zn ANPs on viability of BEAS-2B cells. To determine the cytotoxicity of Cu–Zn ANPs, BEAS-2B cells were exposed to serial concentrations of Cu–Zn ANPs. Untreated cells served as a control group.

XTT assay was performed by using a Cell Viability Assay Kit, which detects the cellular metabolic activities due to colorimetric features. During the assay, the yellow tetrazolium salt XTT is reduced to a highly colored formazan dye by dehydrogenase enzymes in metabolically active cells. This conversion only occurs in viable cells and thus, the amount of formazan produced is proportional to viable cells in the sample (Scudiero et al., 1988; Berridge et al., 2005). Five thousand cells were seeded in into a flat-bottom 96-well plate (which contains 100–200 μl/well culture medium) in triplicate and allowed to grow for 24 h. Cells were than treated with serial concentrations of Cu–Zn ANPs (0.1, 0.5, 1, 5, 8, 12, 16, 20, 25, 50 and 100 μg/ml) for 24 h. Three wells containing 100 μl of growth medium were used for blank absorbance readings. Then 50 μl of the Activated-XTT Solutions were added to each well. Finally, the plate was incubated for 2 h and absorbance was read at 450 nm. Experiments were repeated for three times.

Clonogenic assay, which measures the reduction in plating efficiency in the treatment and control groups, was also used to assess cytotoxicity (Wise et al., 2010). Fifty thousand cells were seeded in T25 tissue culture treated flasks and allowed to grow for 48 h. The cultures were then treated for 24 h with serial concentrations (0.1, 0.5, 1, 5, 8, 12, 16, 20, 25, 50 and 100 μg/ml) of Cu–Zn ANPs. Following exposure period, the treatment medium was collected, the cells were rinsed with PBS; and then removed with 0.25% trypsin/1 mM EDTA solution. Cells were centrifuged at 1000 rpm, 4 °C for 5 min. The pellet was re-suspended in 5 ml of medium, counted with Cedex XS (Roche) cell counter, and re-seeded at colony forming density (500 cells per well) into four pieces of a 60 × 15 mm petri dishes. Colonies were allowed to grow for 7 days, fixed with 100% methanol, stained with crystal violet, and counted. Experiments were repeated for three times.

2.7. Cytokinesis-block micronucleus test

Cytokinesis-block micronucleus test was used to detect chromosomal damages occurred due aneugenic or clastogenic effects (Fenech, 1993). BEAS-2B cells were seeded in T25 tissue culture treated flasks at a density of 3×10^4 cells/flask and allowed to grow for 48 h. Cells were then treated with different concentrations (0.1, 0.2, 0.4, 0.8, 1.6 and 3.2 μg/ml) of Cu–Zn ANPs and H_2O_2 for 24 h. After treatment, cells were further cultured with cytochalasin-B for 24 h. Then, cells were trypsinized centrifuged and resuspended in 0.075 M KCl, and incubated for 2 min. Cells were then fixed 2 times in freshly prepared methanol: glacial acetic acid (3:1). Afterwards, the cell solution was dropped onto pre-cleaned slides and the nucleus was stained by 5% giemsa for 10 min. Slides were investigated under light microscope and the numbers of binucleated (BNC) cells with micronuclei (MNBNC) were recorded based on observation of 2.000 cells per treatment group.

Cytotoxicity was further evaluated by analysis of the nuclear division index (NDI) values. The numbers of cells with one to four nuclei were determined in 1.000 cells. NDI was calculated using the following formula: NDI = (1 × M1 + 2 × M2 + 3 × M3 + 4 × M4)/1.000, where M1 through M4 represent the number of cells with one to four nuclei.

2.8. Alkaline comet assay

Alkaline comet assay was used to detect single stranded DNA damage (Cavas, 2010). BEAS-2B cells were seeded on T25 tissue culture treated flasks at a density of 3×10^4 cells/flask and allowed to grow for 48 h. Cells were then treated with different concentrations (0.1, 0.2, 0.4, 0.8, 1.6 and 3.2 μg/ml) of Cu–Zn ANPs and H_2O_2 for 24 h. After treatments with Cu–Zn ANPs, the alkaline comet assay was performed according to Singh et al. (1988), with some modification (Costa et al., 2008). BEAS-2B cells were harvested and embedded in 0.8% low melting agarose on slides precoated with normal melting point agarose. Slides were then placed in precooled lysis solution (2.5 M NaCl, 0.1 M EDTA, 10 mM Tris base, pH 10) with 1% Triton X for 1 h at 4 °C. Cells were then denatured in alkaline buffer (0.3 M NaCl, 1 mM EDTA) for 30 min in the dark at room temperature (RT). Electrophoresis was performed at 25 V and 300 mA for 20 min. The slides were immersed in neutralization buffer (0.5 M Tris–HCl, pH 7.5) for 10 min followed by dehydration in 70% ethanol. The slides were air dried and stained with ethidium bromide (EtBr). Slides and comets were examined under Nikon epifluorescence microscope equipped with a digical camera (Kameram 21) using an image processing software (Arganit Mikrosistem Comet Assay).

2.9. Immunofluorescence for γ-H2AX foci formation

γ-H2AX foci were used to identify the presence of Cu–Zn ANPs induced double strand DNA breaks (Leopardi et al., 2010) according to the method of Tanaka et al. (2009) with some modifications (Valdiglesias et al., 2011). The cells grown on 8 well chamber slides were exposed to different concentrations (0.1, 0.2, 0.4, 0.8, 1.6 and 3.2 μg/ml) of Cu–Zn ANPs for 24 h. The cells were then fixed in 4% paraformalde-

hyde for 10 min, permeabilized with 0.2% Triton X-100 for 5 min and blocked with 1% BSA for 1 h. Cells were then incubated with anti γ-H2AX antibody at 4 °C overnight and incubated with a AlexaFluor 488-conjugated second antibody for 1 h. Nuclei were counter stained with DAPI. The slides were evaluated under a Nikon Fluorescence Microscope and γ-H2AX foci were counted in 100 cells per treatment.

2.10. Measurement of intracellular ROS formation

The intracellular ROS was determined by using The OxiSelect™ Intracellular ROS Assay Kit. Cells were grown in a 96-well cell culture plate and then pre-incubated with DCFH-DA, which was cell-permeable. ROS were determined in BEAS-2B cells exposed to different concentrations (0.1, 0.2, 0.4, 0.8, 1.6, 3.2 and 6.4 μg/ml) of Cu–Zn ANPs for 3 h. After incubation, the cells were read on a standard fluorescence plate reader. The ROS contents were determined by comparison with the predetermined DCF standard curve.

2.11. Apoptosis and necrosis

2.11.1. M30 assay

Apoptosis was assayed by measuring the level of caspase-cleaved keratin 18 (ccK18, M30) by a commercially available immunoassay kit (M30-Cytodeath ELISA kit, Peviva AB, Sweden) according to the manufacturer's instructions. Cells were seeded into a 96-well plate at a density of five thousand cells per well and incubated for 24 h. At the end of incubation, old medium was removed and cells were washed with PBS and then fresh medium was added (200 μl/well). Cells were exposed by Cu–Zn ANPs with varied concentrations (1.6, 3.2, 6.4 and 16.2 μg/ml) and positive control group (26.56 μM of Cis-platin) for 24 h. The plate was freezed to −20 °C for 6 h and thawed tat room temperature (RT) before the experiments. Then 10 μl 10% Triton-X was added into per well and shaked for 5 m at RT to allow lysis. Subsequently, 2 × 25 μl of the medium/lysate were transferred to the wells of the M30 CytoDeath Coated Microstrips and 75 μl of diluted M30 CytoDeath HRP conjugate was added. Plates were shaked 4 h at RT and washed with wash solution for five times. TMB Substrate was added and incubated for 20 m at RT in dark. Finally, 50 μl stop solution were added and absorbances were read at 450 nm.

2.11.2. M65 assay

Total ratio of cell death based on the measurement of soluble keratin 18 released from dying cells was evaluated using M65 ELISA kit (Peviva AB, Sweden). Cells were seeded into a 96-well plate at a density of five thousand cells per well and incubated for 24 h. At the end of incubation period, old medium was removed and cells were washed with PBS and fresh medium was added (200 μl/well). Cells were exposed to Cu–Zn ANPs with varied concentrations (1.6, 3.2, 6.4 and 12.8 μg/ml) and to 147 μM of H_20_2 (positive control) for 24 h. After lysis, 2 × 25 μl of the medium/lysate was transferred to the wells of the M65 ELISA Coated Microstrips with 75 μl of diluted M65 ELISA HRP conjugate. Plates were shaked 2 h at room temperature and washed with wash solution for five times. TMB Substrate was added and incubated for 20 m at RT in darkness. Finally, 50 μl stop solution were added and absorbance were read at 450 nm.

2.12. Statistical analyses

All the data are represented as means ± SE of three identical experiments carried out in three replicate. Statistical analyses were performed using SPSS 15.0 software. Statistical significance was determined by one-way analysis of variance (ANOVA) followed by Dunnett's multiple comparison tests. Significance was ascribed at $P < 0.05$. The associations between two variables were analyzed by Spearman's correlation. Regression analyses were performed to determine the dose–response relationships.

3. Results

3.1. Nanoparticle characterization

Cu–Zn ANPs zeta potential value of the suspension was determined as −22 mV indicating the stability of solution. This value positively shifted to −17 mV in RPMI-1640 medium. Dynamic Light Spectrophotometer (DLS) and TEM analysis were showed that the particle size was approximately 200 nm and 180 nm, respectively (Fig. 1). The observed size differences between TEM and DLS results could be due to hydratation spheres surrounding the particles in aqueous DLS samples. After Incubation in RPMI-1640 medium an increase in the average size of Cu–Zn ANPs (250 nm) was observed, possibly due to aggregation.

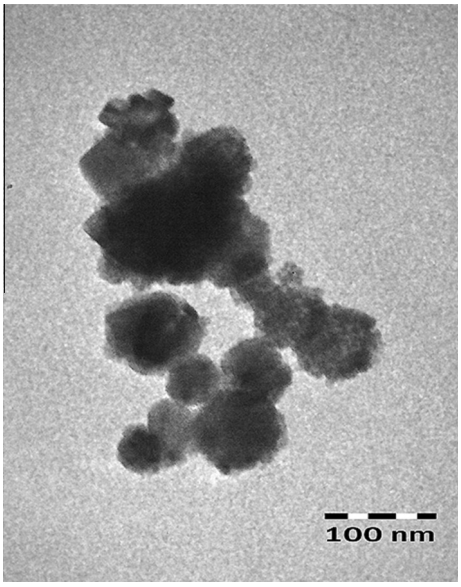

Fig. 1. TEM figures of Cu–Zn ANPs.

3.2. Intracellular uptake

TEM image of a BEAS-2B cell exposed to Cu–Zn ANPs is shown in Fig. 2. TEM evaluation of BEAS-2B cells indicated that Cu–Zn ANPs were taken up by cells and were mainly entrapped in cytoplasm. Although the observed mean particle size determined by DLS is about 200 nm, the evaluation BEAS-2B cells under TEM, indicated that the presence of nanoparticles smaller then 100 nm.

3.3. Cellular viability

XTT and clonogenic assays were used to evaluate the cytotoxicity of Cu–Zn ANPs. Both tests showed that the Cu–Zn NAPs induced dose dependent ($p < 0.01$) cytotoxicity Fig. 3A and B. Based on the dose–response curve 50% inhibitory concentration (IC50) of Cu–Zn ANPs were determined. The average IC50 values were 4.55 μg/mL and 4.66 μg/mL according to XTT test and clonogenic assay, respectively. The obtained IC50 values were compatible between clonogenic and XTT assay results.

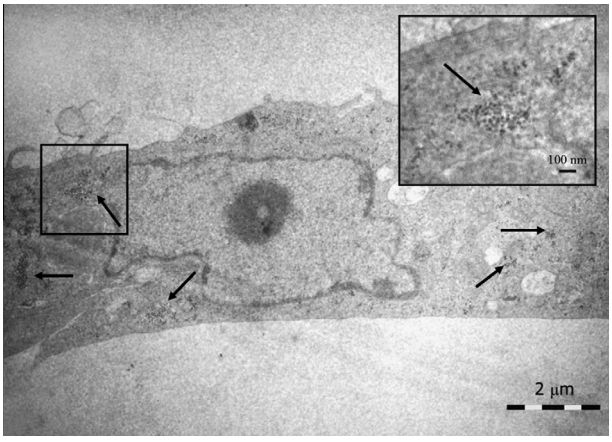

Fig. 2. TEM images showing intracellular localisation of Cu–Zn ANPs. The insert shows magnified view of the selected area.

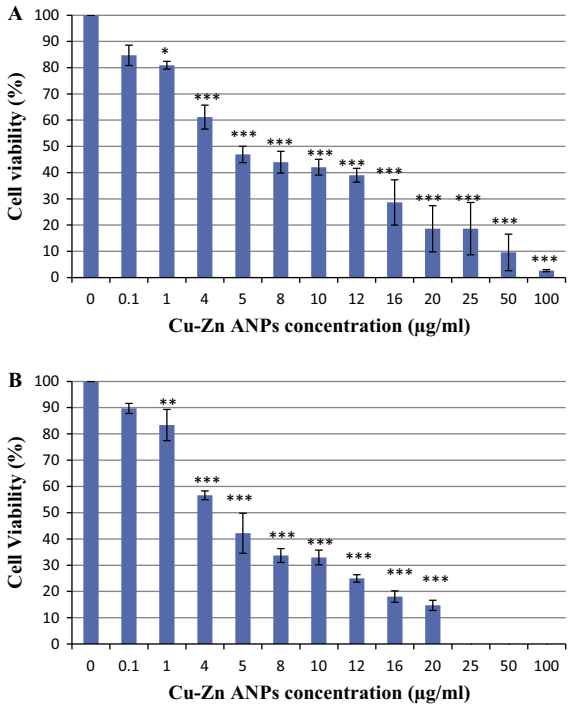

Fig. 3. Viability of BEAS-2B cells treated with Cu–Zn ANPs for 24 h. Results from XTT assay (A) and clonogenic assay (B). Data represent the average of three independent clonogenic assay and XTT assay. Error bars = standard deviation of the mean. Asterisk = significantly different from the control ($^{*}P < 0.05$, $^{**}P < 0.01$, $^{***}P < 0.001$).

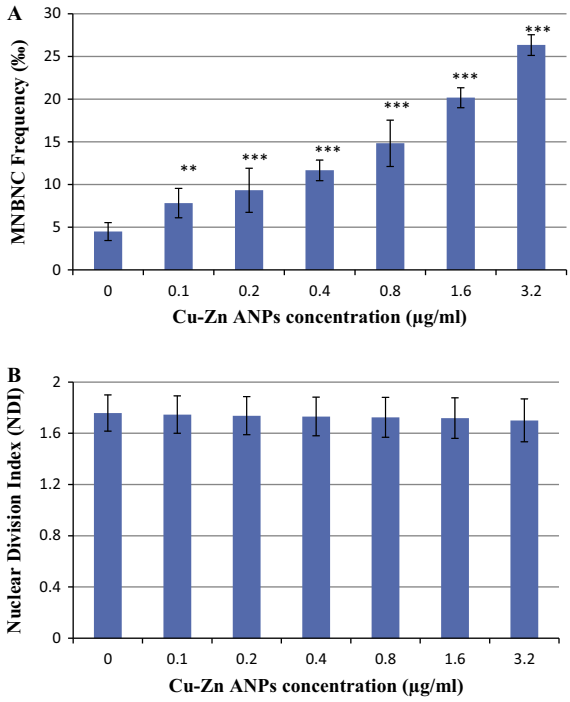

Fig. 4. Graphs showing concentration–response of ‰ MNBN cells (A), nuclear division index (B). Data represent the average of three independent experiments in BEAS-2B cells treated with Cu–Zn ANPs for 24 h. Error bars = standard deviation of the mean. Asterisk = significantly different from the control ($^{**}p < 0.01$, $^{***}p < 0.001$).

3.4. Cytokines-blocked micronucleus test

The micronucleated binucleated cells (MNBNC) frequencies and nuclear division index (NDI) values are summarized in Table 1. The control group frequency of MNBNC was determined as 4.5‰. The MNBNC frequency was increased to 96.16‰ in the H_2O_2 (147 µM) positive control group. 0.2 µg/ml of Cu–Zn ANPs was caused about two fold increase in MNBNC frequency ($p < 0.01$). Moreover, all the other concentrations of Cu–Zn ANPs were also significantly increased the frequency of MNBNC to 11.6‰ (0.4 µg/ml), 14.83‰ (0.8 µg/ml), 20.16‰ (1.6 µg/ml) and 26.33‰ (3.2 µg/ml) (Table 1). Consequently, this increase of micronucleus formation was related with the concentration of NPs ($R^2 = 0.899$; $p \leqslant 0.001$) (Fig. 4a). Results of NDI analyses were shown in Table 1. Treatment with Cu–Zn ANPs was decreased the NDI values at all used concentrations. However these decreases were not statistically significant ($p > 0.05$) (Fig. 4b).

Table 1
Effects of Cu–Zn ANPs on the frequencies of micronucleated binucleated cells (MNBN ‰) and nuclear division index (NDI) values in BEAS-2B cells.

Groups	Concentration	MNBN (‰) ± SE	NDI ± SE
Control	–	4.5 ± 1.048	1.757 ± 0.141
Solvent	3.2 µl/ml	5.17 ± 1.169	1.758 ± 0.142
H_2O_2	147 µM	96.16 ± 1.722***	1.292 ± 0.093
Cu–Zn ANPs	0.1 µg/ml	7.83 ± 1.722**	1.745 ± 0.145
	0.2 µg/ml	9.3 ± 2.581***	1.737 ± 0.148
	0.4 µg/ml	11.6 ± 1.211***	1.730 ± 0.151
	0.8 µg/ml	14.83 ± 2.714***	1.724 ± 0.156
	1.6 µg/ml	20.16 ± 1.169***	1.718 ± 0.158
	3.2 µg/ml	26.33 ± 1.211***	1.7 ± 0.167

*Statistical difference from control $P < 0.05$.
** Statistical difference from control $P < 0.01$.
*** Statistical difference from control $P < 0.001$.

3.5. Alkaline comet assay

Single stand DNA breaks were obtained by comet assay. Tail length, % tail DNA, and olive tail moment values in BEAS-2B cells treated with Cu–Zn ANPs are shown in Table 2. All tested groups were compared based on tail length, % tail DNA and olive tail moment by ANOVA test. All these parameters were related with concentration-dependent ($p < 0.05$). As a result of regression analysis, tail length, % tail DNA and olive tail moment were significantly and concentration dependently increased, $R^2 = 0.727$, $P \leqslant 0.001$; $R^2 = 0.78$, $P \leqslant 0.001$; $R^2 = 0.639$, $p \leqslant 0.001$, respectively (Fig. 5a–c).

3.6. γ-H2AX foci formation

DNA double strand breaks were determined as the formation of γ-H2AX foci. Our results showed that the number of γ-H2AX foci per cell significantly and concentration dependently increased ($R^2 = 0.850$; $p \leqslant 0.001$) following exposure to Cu–Zn ANPs. No significant difference between control and 0.1 µg/ml dose group ($p > 0.05$) observed, however the differences between control and other treatment groups (0.2–3.2 µg/ml) were statistically significant ($p < 0.001$) (Fig. 6).

3.7. Intracellular ROS formation

The potential of Cu–Zn ANPs to induce oxidative stress was assessed by measuring the ROS levels in BEAS-2B cells (Fig. 7). Cu–Zn ANPs significantly induced the intracellular production of ROS in BEAS-2B cells. Statistical analyses showed no significant difference between control group and the lowest dose of 0.1 µg/ml ($p > 0.05$). On the other hand, significant differences between control and other dose groups were observed (0.2, 0.4, 3.2 and 6.4 µg/ml, $p < 0.05$; 0.8, 1.6 µg/ml, $p < 0.01$).

Table 2
Comet assay results in BEAS-2B cells exposed to Cu–Zn ANPs.

Groups	Concentration	Tail length ± SE	% Tail DNA ± SE	Olive tail moment ± SE
Control	–	8.2 ± 1.923	8.799 ± 2.030	1.6 ± 0.894
Solvent	3.2 µl/mL	10 ± 4.358	9.700 ± 1.623	2 ± 1.224
H_2O_2	147 µM	44.4 ± 10.382***	37.859 ± 8.330***	15 ± 6***
Cu–Zn ANPs	0.1 µg/ml	18.6 ± 5.941	17.385 ± 2.724*	5 ± 2.120
	0.2 µg/ml	22.2 ± 7.886*	19.151 ± 2.667**	5.6 ± 2.07
	0.4 µg/ml	23.4 ± 6.348*	22.669 ± 3.491***	6.2 ± 2.580
	0.8 µg/ml	27.8 ± 9.038**	26.879 ± 4.317***	9 ± 3.464***
	1.6 µg/ml	33.8 ± 8.497***	31.116 ± 6.686***	10.8 ± 3.962***
	3.2 µg/ml	37.2 ± 8.613***	36.304 ± 8.129***	12.2 ± 2.774***

* Statistical difference from control $P < 0.05$.
** Statistical difference from control $P < 0.01$.
*** Statistical difference from control $P < 0.001$.

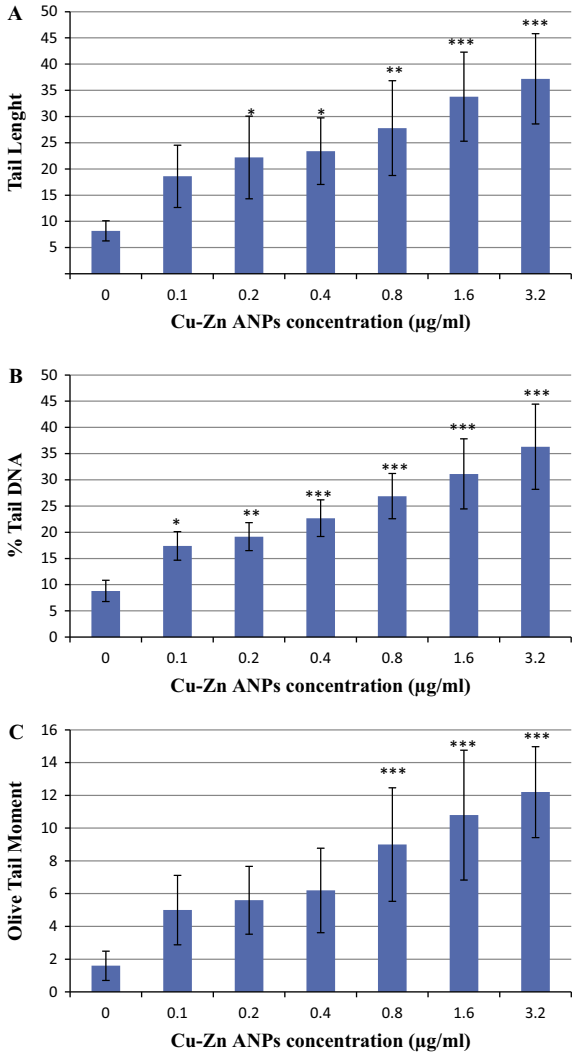

Fig. 5. Graphs showing results of Comet assay in BEAS-2B cells treated with Cu–Zn ANPs for 24 h. Tail length (A), % tail DNA (B), Olive tail moment (C). Data represent the average of three independent experiments. Error bars = standard deviation of the mean. Asterisk = significantly different from the control ($^{*}p < 0.05$, $^{**}p < 0.01$, $^{***}p < 0.001$).

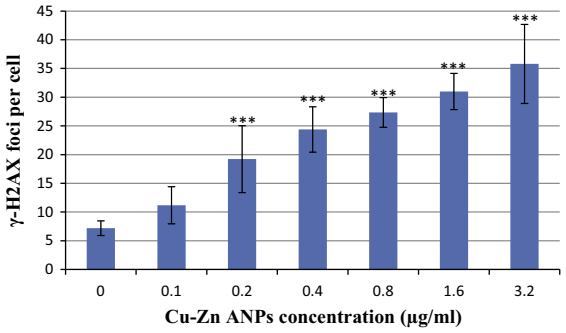

Fig. 6. Graphs showing concentration–response of γ-H2AX foci formation per cell in BEAS-2B cells treated with Cu–Zn ANPs for 24 h. Data represent the average of two independent experiments. Error bars = standard deviation of the mean. Asterisk = significantly different from the control ($^{***}p < 0.001$).

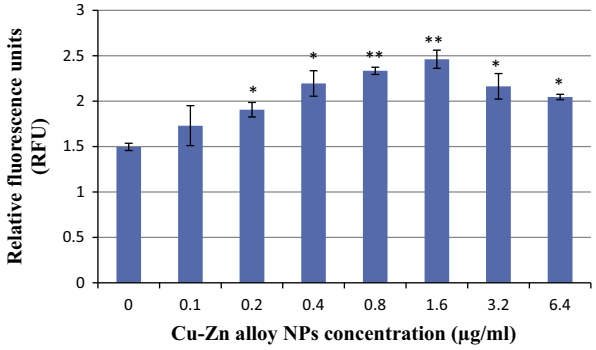

Fig. 7. Effect of Cu–Zn ANPs on ROS generated in BEAS-2B cells. Cells were exposed to different concentrations of Cu–Zn ANPs for 3 h. Data represent the average of two independent experiments. Error bars = standard deviation of the mean. Asterisk = significantly different from the control ($^{*}p < 0.05$, $^{**}p < 0.01$).

3.8. M30 apoptosis and M65 necrosis

Results obtained from M30 apoptosis assay are shown in Fig. 8A. As shown in the figure, treatment with Cu–Zn ANPs slightly increased the apoptosis however these increases were not statistically significant ($p > 0.05$). On the other hand, in M65 necrosis assay significant differences were observed between control and 3.2 µg/ml ($p < 0.05$), 6.4 µg/ml and 12.8 µg/ml ($p < 0.01$) treatment groups (Fig. 8B). Regression analysis indicated that these increases were concentration depended ($R^2 = 0.936$; $p < 0.05$). High percentage of M30/M65 ratios indicates cell death is mainly due to apoptosis (Linder et al., 2010). Therefore M30/M65 ratios were also evaluated and the results are shown in Fig. 8C. We observed that, 50.2% of total cells died by apoptosis and the rest 49.8% by necrosis in the control group. The ratio of cells which died via apoptosis were determined as 41.56%, 38.51%, 35.24%, and 31.49% in 1.6, 3.2, 6.4 and 12.8 µg/ml treatment groups, respectively.

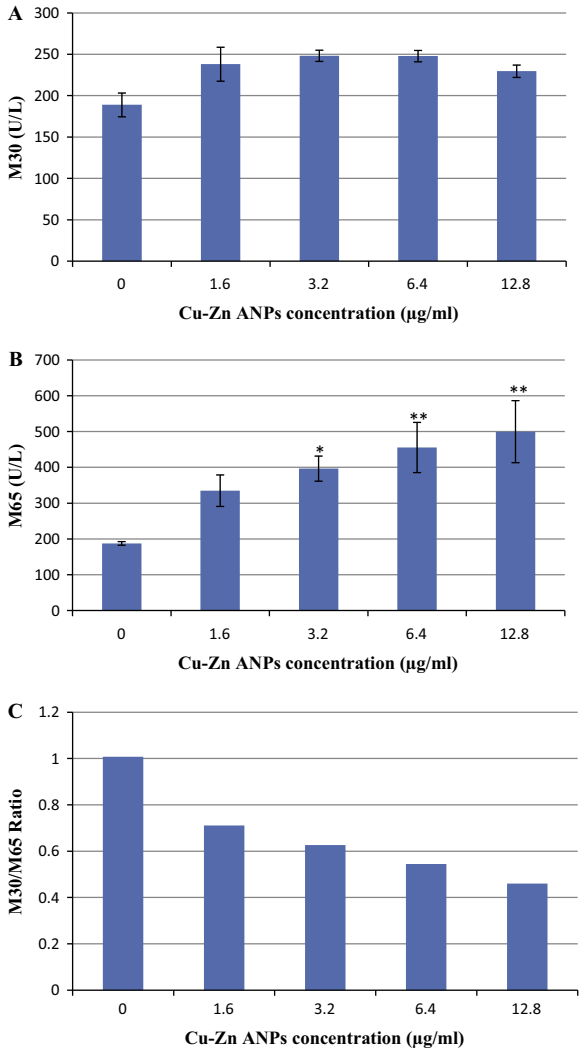

Fig. 8. Graphs showing to Cu–Zn ANPs induced cell death modalities in BEAS-2B cells treated with Cu–Zn ANPs for 24 h. (A) M30 test results, (B)M65 test results and (C) M30/M65 ratios. Data represent the average of three independent experiments. Error bars = standard error of the mean ($N = 6$). Asterisk = significantly different from the control ($^{*}p < 0.05$, $^{**}p < 0.01$).

4. Discussion

The present study provides an evidence for the cytotoxic and genotoxic effects of Cu–Zn ANPs on BEAS-2B cells. To our knowledge, this is the first study dealing with the in vitro genotoxicity Cu–Zn ANPs. Today, it is not exactly known which features of nanoparticles can influence their toxicity; thus the proper characterization of nanoparticles is necessary prior to their toxicity evaluation (Jiang et al., 2009). Therefore, the first step of our study involved the characterization of Cu–Zn ANPs on the basis of shape, size, and stability via TEM, zeta potential and DLS analyses. Our measurements showed that the shape and average size of Cu–Zn ANPs were spherical and 200 nm. Moreover, zeta potential analysis revealed that Cu–Zn ANPs were stable.

Previous studies indicated that metal nanoparticles could induce cytotoxicity. For example, Karlsson et al. (2008) compared the toxicity of different metal oxide particles such as CuO, ZnO, TiO_2, $CuZnFe_2O_4$, Fe_3O_4 and Fe_2O_3 using trypan blue staining and reported that CuO nanoparticles were the most potent regarding cytotoxicity. Furthermore, toxicity evaluation SiO_2, Fe_2O_3 and CuO nanoparticles on Hep-g2 cells revealed that CuO was the most toxic (Fahmy and Cormier, 2009). Moreover, Ahamed et al. (2010) showed the cytotoxic effects of CuO nanoparticles in lung epithelial cells using MTT, NRU and LDH assays. ZnO nanoparticles were also previously reported to induce cytotoxicity in different cell lines such as Caco-2 (Chang et al., 2012), L-132 (Sahu et al., 2013), SHSY5Y (Valdiglesias et al., 2013), as well as HEpG2, A549 and BEAS-2B cells (Akhtar et al., 2012). In addition to the effects of single nanoparticles, Karlsson et al. (2013) comparatively studied the toxicity of Cu, CuO and Cu–Zn particles using trypan blue staining and reported that treatment with Cu and Cu–Zn particles at a concentration of 20 µg/mL induced membrane damage on A549 cells, in 4 h, whereas CuO was not toxic.

In our study, we used the XTT and clonogenic assays to investigate the mitochondrial activity and plating efficiency of cells as indicators of cytotoxicity. We observed that treatment with Cu–Zn ANPs significantly decreased the viability of BEAS-2B cells. The previously reported 24 h IC50 values for Cu nanoparticles were 9.9 µg/mL for RAW 264.7 cells and 12.10 µg/mL for human peripheric lymphocytes (Di Bucchianico et al., 2013) as well as 6.46 µg/mL for A549 cells (Lanone et al., 2009). Similar results were reported for Zn nanoparticles as 13.6 µg/mL for A549 cells (Lin et al., 2009) and 15.55 µg/mL for CaCo-2 cells (Kang et al., 2013). Our experiments on BEAS-2B cells revealed IC50 values of 4.5 and 4.66 µg/mL in XTT test and clonogenic assay, respectively. Our findings are in agreement with those of previous studies, reported reduced cellular viability following exposure to metal nanoparticles.

Copper and zinc containing nanoparticles have also been shown to induce genotoxic damage in different cell lines. Perreault et al. (2012) studied the genotoxic effects of CuO nanoparticles using micronucleus test and reported that treatment with 12.5 µg/mL CuO NP for 24 h significantly increased the micronucleus frequencies in mouse Neuro-2A cells. Similar results were also observed in RAW 264.7 cells and peripheral blood lymphocytes exposed to CuO nanoparticles at concentrations of 0.1–10 µg/mL (Di Bucchianico et al., 2013). Furthermore, Valdiglesias et al. (2013) showed the induction of genotoxic damage in human SHSY5Y neuronal cells, exposed to ZnO nanoparticles at concentrations of 20–30 µg/mL for 6 h, using the micronucleus and gH2AX foci assays.

In the present study, we investigated the genotoxic effects of Cu–Zn ANPs (0.1–3.2 µg/mL) on BEAS-2B lung epithelial cells the using micronucleus, comet and H2AX assay test systems. We observed significant increases in the frequencies of micronucleated cells following exposure to Cu–Zn ANPs. Our comet assay results further indicated that Cu–Zn ANPs were able to induce single stranded DNA damage, as demonstrated by dose dependent increase in tail length, % DNA tail and olive tail moment values. An additive method, which was convenient to determine DNA damaging effects, is the evaluation of γ-H2AX foci formations. In this study, we evaluated the average number of γ-H2AX foci per cell and found significant dose dependent increases following exposure to Cu–Zn ANPs. Overall, our genotoxicity findings are in agreement with those of previous reports. Considering the previously reported IC50 values and the tested concentrations mentioned above, it is possible to suggest that Cu–Zn ANPs are more toxic than its single components. However, these findings might also be due to different responses shown by different cell types or even the media used (Bumgardner et al., 1989).

Results of previous studies suggested that excessive production of ROS and oxidative stress could be one of the possible mechanisms of nanoparticle toxicity (Ahamed et al., 2011; Akhtar et al., 2012). For instance, exposure to CuO nanoparticles, at concentrations ranging form 10 to 50 µg/mL for 24 h, was shown to induce oxidative stress in A549 human lung cells (Ahamed et al., 2010). Similar results were obtained in CaCo-2 cells treated with 6.2, 12.5, 25 and 100 µg/mL concentrations of ZnO nanoparticles for

24 h (Kang et al., 2013). In our study, we observed that exposure to Cu–Zn ANPs (0.2–6.2 μg/mL) increased intracellular ROS formation in BEAS-2B cells. In aqueous suspensions, either release of Zn and Cu ions or nanoparticle itself could cause oxidative damage (Hann et al., 2012; Karlsson et al., 2013). Our TEM analyses revealed cytoplasmic localization of Cu–Zn ANPs smaller than 100 nm. Upon entering the cell, particles may induce intracellular oxidative stress by disturbing the balance between oxidant and anti-oxidant processes. We suggest that nanoparticles are taken up by the cells might led to increased production of ROS and ultimately apoptotic and necrotic cell death. Consequently, our results are compatible with those of previous studies evaluated the toxicity of different nanoparticles using ROS formation and oxidative stress (Chang et al., 2012; Manke et al., in press).

In previous studies it was concluded that nanoparticles might lead to the cell death by apoptosis or necrosis. For instance, Alarifi et al. (2013) reported that 24 h treatment with 5, 10 and 20 μg/mL concentrations of CuO nanoparticles significantly induced onset of apoptosis in human skin epidermal cells. Similarly, Kang et al. (2013) reported that 24 h treatment of CaCo-2 cells with 12.5 and 50 μg/mL concentrations ZnO nanoparticles induced apoptosis and necrosis, respectively. In our study, we used M30 apoptosis and M65 necrosis elisa tests to analyze cell death pathway in BEAS-2B cells treated with Cu–Zn ANPs. Our results revealed that Cu–Zn ANPs induced slight amount apoptosis and high amount of necrosis in parallel to increased concentrations. Similar results were reported by Jeng and Swanson (2006) in mouse neuroblastoma cells treated with ZnO nanoparticles. They observed small percentage of apoptotic cells (15%) at low concentration (25 μg/mL) and almost total necrosis at high concentration (100 μg/mL).

In conclusion, our results first demonstrated that Cu–Zn ANPs possess cytotoxic and genotoxic potential in human lung epithelial cells (BEAS-2B). Although additional studies are required to further explain specific mechanisms underlying the cyto-genotoxicity of Cu–Zn ANPs, our findings indicate that intracellular ROS can play an important role in their toxicity. Further comparative studies could also provide valuable insight regarding the toxicity of alloy nanoparticles and their components. This will be important to obstruct serious problems on environment and health; finally lead to the development of conservation strategies.

Conflict of Interest

The authors declare that there are no conflicts of interest.

Transparency Document

The Transparency document associated with this article can be found in the online version.

Acknowledgements

This study was supported by Uludag University Scientific Research Fund (Project No. KUAP F-2012/61). The authors are indebted to Uludag University for its financial support of the study. This study was made from PhD thesis by Ümit Kumbıçak at Uludag University.

References

Adamcakova-Dodd, A., Stebounova, L.V., Kim, J.S., Vorrink, S.U., Ault, A.P., O'Shaughnessy, P.T., Grassian, V.H., Thorne, P.S., 2014. Toxicity assessment of zinc oxide nanoparticles using sub-acute and sub-chronic murine inhalation models. Part. Fibre Toxicol. 11, 1–15.

Ahamed, M., Siddiqui, M.A., Akhtar, M.J., Ahmad, I., Pant, A.B., Alhadlaq, H.A., 2010. Genotoxic potential of copper oxide nanoparticles in human lung epithelial cells. Biochem. Biophys. Res. Commun. 396, 578–583.

Ahamed, M., Akhtar, M.J., Siddiquic, M.A., Ahmad, J., Musarrat, J., Al- Khedhairy, A.A., AlSalhi, M.S., Alrokayan, S.A., 2011. Oxidative stress mediated apoptosis induced by nickel ferrite nanoparticles in cultured A549 cells. Toxicology 283, 101–108.

Akhtar, M.J., Ahamed, M., Kumar, S., Khan, A.M., Ahmad, J., Alrokayan, S.A., 2012. Zinc oxide nanoparticles selectively induce apoptosis in human cancer cells through reactive oxygen species. Int. J. Nanomed. 7, 845–857.

Alarifi, S., Ali, D., Verma, A., Alakthani, S., Ali, B.A., 2013. Cytotoxicity and genotoxicity of copper oxide nanoparticles in human skin keratinocytes cells. Int. J. Toxicol. 32, 296–307.

Amara, S., Slama, I.B., Mrad, I., Rihane, N., Khemissi, W., El Mir, L., Rhouma, K.B., Abdelmelek, H., Sakly, M., 2014. Effects of zinc oxide nanoparticles and/or zinc chloride on biochemical parameters and mineral levels in rat liver and kidney. Hum. Exp. Toxicol., in press, http://dx.doi.org/10.1177/0960327113510327.

Arora, S., Rajwade, J.M., Paknikar, K.M., 2012. Nanotoxicology and in vitro studies: the need of the hour. Toxicol. Appl. Pharmacol. 258, 151–165.

Ateş, M., Arslan, Z., Demir, V., Daniels, J., Farah, I.O., 2014. Accumulation and toxicity of CuO and ZnO nanoparticles through waterborne and dietary exposure of goldfish (*Carassius auratus*). Environ. Toxicol., in press, http://dx.doi.org/10.1002/tox.22002.

Bardack, S., Dalgart, C.L., Kalinich, J.F., Kasper, C.E., 2014. Genotoxic changes to rodent cells exposed in vitro to tungsten, nickel, cobalt and iron. Int. J. Environ. Res. Public Health 11 (11), 2922–2940.

Berridge, M.V., Herst, P.M., Tan, A.S., 2005. Tetrazolium dyes as tools in cell biology: new insights into their cellular reduction. Biotechnol. Annu. Rev. 11, 127–152.

Bondarenko, O., Juganson, K., Ivask, A., Kasemets, K., Mortimer, M., Kahru, A., 2013. Toxicity of Ag, CuO and ZnO nanoparticles to selected environmentally relevant test organisms and mammalian cells in vitro: a critical review. Arch. Toxicol. 87, 1181–1200.

Bumgardner, J.D., Lucas, L.C., Tilden, A.B., 1989. Toxicity of copper-based dental allot in cell culture. J. Biomed. Mater. Res. 23, 1103–1114.

Buzea, C., Blandino, I.P., Robbie, K., 2007. Nanomaterials and nanoparticles: sources and toxicity. Biointerphases 2, 17–71.

Capasso, L., Camatini, M., Gualtieri, M., 2014. Nickel oxide nanoparticles induce inflammation and genotoxic effects in lung epithelial cells. Toxicol. Lett. 226, 28–34.

Cavas, T., 2010. In vivo genotoxicity evaluation of atrazine and atrazine-based herbicide on fish *Carassius auratus* using the micronucleus test and the comet assay. Food. Chem. Toxicol. 49, 1431–1435.

Chang, Y.N., Zhang, M., Xia, L., Zhang, J., Xing, G., 2012. The toxic effects and mechanisms of CuO and ZnO nanoparticles. Materials 5, 2850–2871.

Costa, S., Coelho, P., Costa, C., Silva, S., Mayan, O., Santos, L.S., Gaspar, J., Teixeira, J.P., 2008. Genotoxic damage in pathology anatomy laboratory workers exposed to formaldehyde. Toxicology 252, 40–48.

Di Bucchianico, S., Fabbrizi, M.R., Misra, S.K., Valsami-Jones, E., Derhanu, D., Reip, P., Bergamaschi, E., Migliore, L., 2013. Multiple cytotoxic and genotoxic effects induced in vitro by differently shaped copper oxide nanomaterials. Mutagenesis 28, 287–299.

Fahmy, B., Cormier, S.A., 2009. Copper oxide nanoparticles induce oxidative stress and cytotoxicity in airway epithelial cells. Toxicol. In Vitro 23, 1365–1371.

Fenech, M., 1993. The cytokinesis-block micronucleus technique and its application to genotoxicity studies in human populations. Environ. Health. Perspec. 101, 101–107.

Ferreira, A.J., Cemlyn-Jones, J., Cordeiro, C.R., 2013. Nanoparticles, nanotechnology and pulmonary nanotoxicology. Rev. Port. Pneumol. 19, 28–37.

Ferrando, R., Jellinek, J., Johnston, R.L., 2008. Nanoalloys: from theory to applications of alloy clusters and nanoparticles. Chem. Rev. 108, 845–910.

Gumus, D., Berber, A.A., Ada, K., Aksoy, H., 2014. In vitro genotoxic effects of ZnO nanomaterials in human peripheral lymphocytes. Cytotechnology 66, 317–325.

Han, X., Geller, B., Moniz, K., Das, P., Chippindale, A.K., Walker, V.K., 2014. Monitoring the developmental impact of copper and silver nanoparticle exposure in Drosophila and their microbiomes. Sci. Total Environ. 487, 822–829.

Hanna, S.K., Miller, R.J., Zhou, D., Keller, A.A., Lenihan, H.S., 2013. Accumulation and toxicity of metal oxide nanoparticles in a soft-sediment estuarine amphipod. Aquat. Toxicol. 143, 441–446.

Hann, A., Fuhirott, J., Loos, A., Barcikowski, S., 2012. Cytotoxicity and ion release of alloy nanoparticles. J. Nanopart. Res. 14, 1–10.

Hussain, S.M., Hess, K.L., Gearhart, J.M., Geiss, K.T., Schlager, J.J., 2005. In vitro toxicity of nanoparticles in BRL 3A rat liver cells. Toxicol. in Vitro 19, 975–983.

Jeng, H.A., Swanson, J., 2006. Toxicity of metal oxide nanoparticles in mammalian cells. J. Environ. Sci. Health. A. Tox. Hazard. Subst. Environ. Eng. 41, 2699–2711.

Jiang, J.K., Oberdörster, G., Biswas, P., 2009. Characterization of size, surface charge, and agglomeration state of nanoparticle dispersions for toxicological studies. J. Nanopart. Res. 11, 77–89.

Kang, T., Guan, R., Xiaqiang, C., Song, y., Jiang, H., Zhao, J., 2013. In vitro toxicity of different-sized ZnO nanoparticles in Caco-2 cells. Nano Res. Lett. 8, 496.

Karlsson, H.L., Cronholm, P., Gustafsson, J., Möller, L., 2008. Copper oxide nanoparticles are highly toxic: a comparison between metal oxide nanoparticles and carbon nanotubes. Chem. Res. Toxicol. 21 (9), 1726–1732.

Karlsson, H.L., Cronholm, P., Hedberg, Y., Tornberg, M., Batticee, L.D., Svedhem, S., Wallinder, I.O., 2013. Cell membrane damage and protein interaction induced

by copper containing nanoparticles-importance of the metal release process. Toxicology 313, 59–69.
Kim, H.R., Kim, M.J., Lee, S.Y., Oh, S.M., Chung, K.H., 2011. Genotoxic effects of silver nanoparticles stimulated by oxidative stress in human normal bronchial epithelial (BEAS-2B) cells. Mutat. Res. 726, 129–135.
Lanone, S., Rogerieux, F., Geys, J., Dupont, A., Maillot-Marechal, E., Boczkowski, J., Lacroix, G., Hoet, P., 2009. Comparative toxicity of 24 manufactured nanoparticles in human alveolar epithelial and macrophage cell lines. Part. Fibre Toxicol. 6, 1–14.
Leopardi, P., Cordelli, E., Villani, P., Cremona, T.P., Conti, L., De Luca, G., Crebelli, R., 2010. Assessment of in vivo genotoxicity of the rodent carcinogen furan: evaluation of DNA damage and induction of micronuclei in mouse splenocytes. Mutagenesis 25, 57–62.
Lin, W., Xu, Y., Huang, C.C., Ma, Y., Shannon, K.B., Chen, D.R., Huang, W.Y., 2009. Toxicity of nano- and micro-sized ZnO particles in human lung epithelial cells. J. Nanopart. Res. 11, 25–39.
Linder, S., Olofsson, H.M., Herrmann, R., Ulukaya, E., 2010. Utilization of cytokeratin-based biomarkers for pharmacodynamic studies. Expert. Rev. Mol. Diagn. 10 (3), 353–359.
Love, S.A., Maurer-Jones, M.A., Thompson, J.W., Lin, Y.S., Haynes, C.L., 2012. Assessing nanoparticle toxicity. Annu. Rev. Anal. Chem. 5, 181–205.
Manke, A., Wang, L., Rojanasakul, Y., 2013. Mechanisms of nanoparticle-induced oxidative stress and toxicity. BioMed. Res. Int., in press, http://dx.doi.org/10.1155/2013/942916:15.
Meruvu, H., Vangalapati, M., Chippada, S.C., Bammidi, S.R., 2011. Synthesis and characterization of zinc oxide nanoparticles and its antimicrobial activity against *Bacillus subtilis* and *Escherichia coli*. Rasayan J. Chem. 4, 217–222.
Midander, K., Cronholm, P., Karlsson, H.L., Elihn, K., Möller, L., Leygraf, C., Wallinder, I.O., 2009. Surface characteristics, copper release, and toxicity of nano- and micrometer-sized copper and copper(II) oxide particles: a cross-disciplinary study. Small 5, 389–399.
Nel, A., Xia, T., Madler, L., Li, N., 2006. Toxic potential of materials at the nanolevel. Science 311 (5761), 622–627.
Perreault, F., Melegari, S.P., Costa, C.H., Rossetto, O.F., Popovic, R., Matias, W.G., 2012. Genotoxic effects of copper oxide nanoparticles in Neuro 2A cell cultures. Sci. Total Environ. 441, 117–124.
Roduner, E., 2006. Size matters: Why nanomaterials are different. Chem. Soc. Rev. 35, 583–592.
Rousk, J., Ackermann, K., Curling, S.F., Jones, D.L., 2012. Comparative toxicity of nanoparticulate CuO and ZnO to soil bacterial communities. Plos One 7, e34197. http://dx.doi.org/10.1371/journal.pone.0034197.
Sahu, D., Kannan, G.M., Vijayaraghavan, R., Anand, T., Khanum, F., 2013. Nanosized zinc oxide induces toxicity in human lung cells. ISRN Toxicol.. http://dx.doi.org/10.1155/2013/316075.
Schrand, A.M., Rahman, M.F., Hussain, S.M., Schlager, J., Smith, D.A., Syed, A.F., 2010. Metal-based nanoparticles and their toxicity assessment. Nanomed. Nanobiotechnol. 2, 544–568.
Scudiero, D.A., Shoemaker, R.H., Paull, K.D., Monks, A., Tierney, S., Nofziger, T.H., Currens, M.J., Seniff, D., Boyd, M.R., 1988. Evaluation of a soluble tetrazolium/formazan assay for cell growth and drug sensitivity in culture using human and other tumor cell lines. Cancer Res. 48, 4827–4833.
Singh, N.P., McCoy, M.T., Tice, R.R., Schneider, E.L., 1988. A simple technique for quantitation of low levels of DNA damage in individual cells. Exp. Cell Res. 175, 184–191.
Singh, N., Mansian, B., Jenkins, G.J.S., Griffiths, S.M., Williams, P.M., Maffeis, T.G.G., Wright, C.J., 2009. Nanogenotoxicology: the DNA damaging potential of engineered nanomaterials. Biomaterials 30, 3894–3914.
Tanaka, T., Halicka, D., Traganos, F., Darzynkiewicz, Z., 2009. Cytometric analysis of DNA damage, phosphorylation of histone H2AX as a marker of DNA double-strand breaks (DSBs). Methods Mol. Biol. 523, 161–618.
Trickler, W.J., Lantz, S.M., Schrand, A.M., Robinson, B.L., Newport, G.D., Schlager, J.J., Paule, G.M., Slikker, W., Biris, A.S., Hussain, S.M., Ali, S.F., 2012. Effects of copper nanoparticles on rat cerebral microvessel endothelial cells. Nanomedicine 7, 835–846.
Tripathi, A., Saravanan, S., Pattnaik, S., Moorthi, A., Partridge, N.C., Selvamurugan, N., 2012. Bio-composite scaffolds containing chitosan/nano-hydroxyapatite/nano-copper–zinc for bone tissue engineering. Int. J. Biol. Macromol. 50, 294–299.
Valdiglesias, V., Laffon, B., Pásaro, E., Méndez, J., 2011. Okadaic acid-induced genotoxicity in human cells evaluated by micronucleus test and γH2AX analysis. J. Toxicol. Environ. Health 74, 980–992.
Valdiglesias, V., Costa, C., Kiliç, G., Costa, S., Pásaro, E., Laffon, B., Teixeira, J.P., 2013. Neuronal cytotoxicity and genotoxicity induced by zinc oxide nanoparticles. Environ. Int. 55, 92–100.
Wahab, R., Kaushik, N.K., Kaushik, N., Choi, E.H., Umar, A., Dwivdi, S., Musarrat, J., Al-Khedhairy, A.A., 2013. ZnO nanoparticles induces cell death in malignant human T98G gliomas, KB and non malignant HEK cells. J. Biomed. Nanotechnol. 9, 1181–1189.
Wise, S.S., Holmes, A.L., Qin, Q., Hong, X., Katsifis, S.P., Thompson, W.D., Wise Sr., J.P., 2010. Comparative genotoxicity and cytotoxicity of four hexavalent chromium compounds in human bronchial cells. Chem. Res. Toxicol. 23, 365–372.